Eur. J. Biochem. **270**, 2543–2556 (2003) © FEBS 2003 doi:10.1046/j.1432-1033.2003.03634.x

THE EMBO LECTURE

On peptide bond formation, translocation, nascent protein progression and the regulatory properties of ribosomes

Delivered on 20 October 2002 at the 28th FEBS Meeting in Istanbul

Ilana Agmon[1], Tamar Auerbach[1,2], David Baram[1], Heike Bartels[3], Anat Bashan[1], Rita Berisio[3,*], Paola Fucini[4], Harly A. S. Hansen[3], Joerg Harms[3], Maggie Kessler[1], Moshe Peretz[1], Frank Schluenzen[3], Ada Yonath[1,3] and Raz Zarivach[1]

[1]*Department of Structural Biology, The Weizmann Institute, Rehovot, Israel;* [2]*FB Biologie, Chemie, Pharmazie, Frei University Berlin, Germany;* [3]*Max Planck Research Unit for Ribosomal Structure, Hamburg, Germany;* [4]*Max Planck Institute for Molecular Genetics, Berlin, Germany*

High-resolution crystal structures of large ribosomal subunits from *Deinococcus radiodurans* complexed with tRNA-mimics indicate that precise substrate positioning, mandatory for efficient protein biosynthesis with no further conformational rearrangements, is governed by remote interactions of the tRNA helical features. Based on the peptidyl transferase center (PTC) architecture, on the placement of tRNA mimics, and on the existence of a two-fold related region consisting of about 180 nucleotides of the 23S RNA, we proposed a unified mechanism integrating peptide bond formation, A-to-P site translocation, and the entrance of the nascent protein into its exit tunnel. This mechanism implies sovereign, albeit correlated, motions of the tRNA termini and includes a spiral rotation of the A-site tRNA-3′ end around a local two-fold rotation axis, identified within the PTC. PTC features, ensuring the precise orientation required for the A-site nucleophilic attack on the P-site carbonyl-carbon, guide these motions. Solvent mediated hydrogen transfer appears to facilitate peptide bond formation in conjunction with the spiral rotation. The detection of similar two-fold symmetry-related regions in all known structures of the large ribosomal subunit, indicate the universality of this mechanism, and emphasizes the significance of the ribosomal template for the precise alignment of the substrates as well as for accurate and efficient translocation. The symmetry-related region may also be involved in regulatory tasks, such as signal transmission between the ribosomal features facilitating the entrance and the release of the tRNA molecules. The protein exit tunnel is an additional feature that has a role in cellular regulation. We showed by crystallographic methods that this tunnel is capable of undergoing conformational oscillations and correlated the tunnel mobility with sequence discrimination, gating and intracellular regulation.

Keywords: ribosomes; peptide bond formation; translocation; tunnel gating; elongation arrest.

Ribosomes, the universal cell organelles responsible for protein synthesis, are giant nucleoprotein assemblies built of two unequal subunits (0.85 and 1.45 MDa in prokaryotes) that associate upon the initiation of protein biosynthesis. Already in the early days of ribosome research peptide bond formation, the principal reaction of protein biosynthesis, was localized in the large ribosomal subunit, and the region assigned to this activity was called the peptidyl transferase center (PTC). Consistently, the crystal structures of the whole ribosome [1] and of the large subunit from both the archaeon *Haloarcula marismortui*, H50S [2–6], and the eubacterium *Deinococcus radiodurans*, D50S [7–10] showed that the PTC is located at the bottom of a V-shaped cavity in the middle of the large subunit. Within this cavity, two highly conserved RNA features, the A- and the P-loops, accommodate the 3′-termini (CCA) of the A (aminoacyl) and the P (peptidyl) tRNAs. The PTC pocket is vacant except for the bases of nucleotides A2602 (*Escherichia coli* numbering system is used throughout the text) and U2585, which bulge into its center, leaving an arched void of a width sufficient to accommodate tRNA-3′ ends. The PTC rear-wall spans from the A- to the P-site, and its bottom serves as an entrance to a very long tunnel along which the nascent proteins progress.

During the course of protein biosynthesis the A-site tRNA carrying the nascent chain, passes into the P-site and the deacylated P-site tRNA acting as the 'leaving group' after peptide bond formation, moves from the P-site to the E (exit)-site. This fundamental process in the elongation cycle, called translocation, is assisted by nonribosomal

Correspondence to A. Yonath, Department of Structural Biology, The Weizmann Institute, 76100 Rehovot, Israel; Max-Planck-Research Unit for Ribosomal Structure, 22603 Hamburg, Germany. Fax: + 972 8 9344154, Tel.: + 972 8 9343028, E-mail: ada.yonath@weizmann.ac.il

Abbreviations: PTC, peptidyl transferase center; ASM, T-arm of tRNA; TAO, troleandomycin.

**Permanent address*: Institute of Biostructure and Bioimage, CNR, 80138 Napoli, Italy.

(Received 16 December 2002, revised 9 April 2003, accepted 24 April 2003)

factors, among them EF-Tu that delivers the aminoacylated tRNA to the A-site and EF-G, which promotes translocation. Translocation may be performed by a shift [11,12] or by incorporating intermediate hybrid states, in which tRNA acceptor stem moves relative to the large subunit whereas the anticodon moves relative to the small one, and the two relative movements are not simultaneous [13,14]. Regardless of the mechanism, the translocation process requires substantial motion of ribosomal components, consistent with the conformations observed for the features known to be involved in various functional tasks of the ribosome in the structures of the bound and unbound large ribosomal subunit [1,7,15]. The significance of the inherent ribosomal mobility is further demonstrated by the disorder of most functionally related features in the H50S structure [2,3] that was determined under far from physiological conditions.

Puromycin, a protein biosynthesis inhibitor that exerts its effect by direct interactions with the PTC, played a central role in many experiments aimed at revealing the molecular mechanism of peptide bond formation. As puromycin structure resembles that of the 3′ terminus of aminoacyl-tRNA, except for the nonhydrolyzable amide bridge that replaces the tRNA ester bond, its binding to the ribosome in the presence of an active donor-substrate can result in the formation of a single peptide bond [16–23]. Nevertheless, despite the wealth of information accumulated over the years and the availability of crystallographically determined high-resolution structures, the molecular mechanism of peptidyl transferase activity is still not completely understood.

Early biochemical and functional studies indicated that the ribosome's contribution to the peptidyl-transferase activity is the provision of a template for precise positioning of the tRNA molecules (e.g. [24–31]). Our crystallographic results, described below and in [7,8,15], are consistent with this interpretation, and suggest that the ribosome provides a template not only for peptide bond formation but also for translocation. The alternative hypothesis, deduced from the crystal structure of H50S in complex with a partially disordered tRNA-mimic and a compound presumed to be a reaction intermediate, claimed that the ribosome participates actively in the enzymatic catalysis of the formation of the peptide bond [3]. This proposal raised considerable doubt, based on biochemical and mutation data [29,32–35]. Indeed, recent analysis of structures of additional complexes of the same particle, H50S, extended these uncertainties, as in these complexes the PTC features that were originally suggested to catalyze peptide bond formation were found to point at a direction opposite to the expected peptide bond [5]. Consequently, a new proposal, consistent with our results [7,8], has been published [36]. Besides positional catalysis, which seems to be the main catalytic activity of the ribosome, ribosomal components may contribute to rate enhancement of the reaction, as suggested by direct kinetic measurements [37].

In order to analyze the tRNA binding modes that lead to biosynthesis of proteins, we chose to focus on the large ribosomal subunit from *D. radiodurans*, an extremely robust eubacterium that shares extensive similarity with *E. coli* and *Thermus thermophilus* [38]. This bacterium was isolated from irradiated canned meat, soil, animal feces, weathered granite, room dust, atomic piles waste and irradiated medical instruments. It was found to survive under DNA-damage-causing conditions, such as hydrogen peroxide and ionizing or ultraviolet radiation, mainly through the ring-like packing of its genome [39]. It was also proven to be suitable for ribosomal crystallography as well-diffracting crystals of its large ribosomal subunit (D50S) could be grown under conditions almost identical to those optimized for high biological activity [7,9,10,15].

Precise substrate positioning is determined by remote interactions

We determined the three-dimensional structures of D50S complexed with several substrate analogs that were designed to mimic the portion of the tRNA molecule that interacts with the large ribosomal subunit within the assembled ribosome. Various analogs were used, ranging in size from short puromycin derivatives to compounds mimicking the entire acceptor stem of tRNA, all of which possess a 3′ ACC-puromycin that corresponds to tRNA bases 73–76. The longest analog is a 35-nucleotide chain that mimics the entire acceptor stem and the T-arm of tRNA (called ASM). The shortest is a four-nucleotide chain, called ACCP [8].

The high-resolution crystal structures of their complexes with D50S indicated that precise positioning of substrates is dictated by remote interactions of the helical stems of tRNA molecules and not by the tRNA-3′ terminus [8]. ASM interacts extensively with the upper part of the PTC cavity. It packs groove-to-backbone with the 23S RNA helix H69, the large subunit component involved in the intersubunit bridge B2a, and forms various contacts with protein L16 (Fig. 1). Originally, based on sequence analysis, no protein was identified in the large ribosomal subunit from *H. marismortui* to be a homolog of the eubacterial protein L16. However, structural similarity between D50S L16 and H50S L10e and their relative locations within the large ribosomal subunit reveled unambiguously that protein L10e is of a prokaryotic, rather than eukaryotic, origin. The preservation of a three-dimensional fold for less related sequences manifests the importance of this fold, as expected from a ribosomal moiety that has a significant contribution to the precise placement of A-site tRNA.

Similar, albeit distinctly different binding modes are formed (Fig. 1) in the absence of remote interactions, either because the substrate analogs are too short for the formation of these interactions, or due to disorder in helix H69, as is the case in the crystal structure of the large ribosomal subunit from *H. marismortui*, H50S [2,3]. None of the various binding modes of those analogs is identical to that of ASM [8], and analyses of these modes indicate that the chemical nature of each analog may dictate the properties of its binding mode. Furthermore, in contrast to ASM [8], the short or loosely placed analogs are positioned with orientations requiring conformational rearrangements in order to participate in peptide bond formation [3,5,6]. These rearrangements are bound to consume time, which might explain the low rate of peptidyl bond formation by short puromycin derivatives.

The PTC is inherently flexible

Variability in the PTC conformation, observed despite its high sequence conservation, could be correlated not

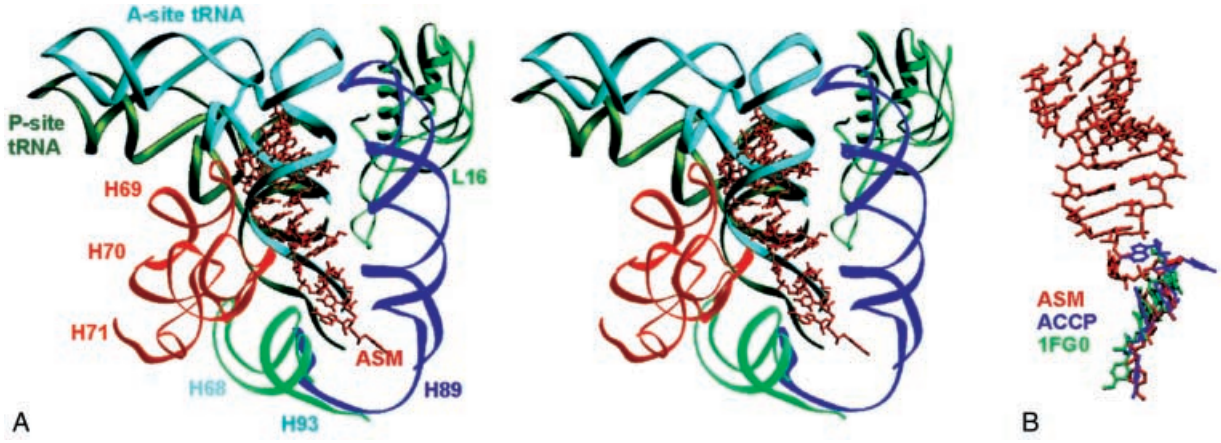

Fig. 1. The PTC pocket. (A) A stereo view, showing the PTC in D50S and includes the docked A- and P-site tRNAs (ribbon representation in cyan and olive-green, respectively), ASM (shown as red atoms). It highlights the major contributions of H69 and protein L16 to the precise positioning of ASM, a 35 nucleotides tRNA acceptor stem mimic [8]. (B) The location of two puromycin derivatives, 1FGO in H50S [3] and ACCP [8] in D50S, superimposed on ASM [8]. Note the similarities and the differences between the various orientations.

only with phylogenetic variations [22], but also with the functional state of the ribosome. Thus, nucleotides showing different orientations in the T70S-tRNAs complex and the liganded H50S were identified [1]. In addition, findings, accumulated over more than three decades, indicate that variations of chemical conditions induce substantial conformational changes in the PTC of *E. coli* ribosomes [33,40]. Some of the variations in the PTC conformations of D50S and H50S crystal structures could be correlated consistently with the deviations of the crystal environments from the physiological conditions. Interestingly, despite the differences in binding modes, the Watson–Crick base-pair between the PTC base G2553 and tRNA-C75 [41] is formed by all of the large subunit complexes [3,5,6], as well as by the A-site tRNA [1] docked from the 5.5 Å structure of the entire ribosome onto D50S [7].

The diversity of the PTC binding modes observed in the different crystal forms indicates that the PTC tolerates various orientations of short puromycin derivatives (Fig. 1). It is likely that the inherent flexibility of the PTC assists the conformational rearrangements required for substrate analogs that are bound in a nonproductive manner for peptide bond formation. The inherent flexibility of the PTC is demonstrated also by the action of the antibiotic sparsomycin, a potent ribosome-targeted inhibitor with a strong activity on all cell types, including Gram-positive bacteria and highly resistant archae [23,42,43]. We found that sparsomycin binds to the large ribosomal subunit solely through stacking interactions with the highly conserved base A2602 [8], consistent with cross-linking data [44] and rationalizing the difficulties of its localization [18,23,44,45]. In accordance with the finding that despite sparsomycin universality, ribosomes from various kingdoms display differences in binding affinities to it [46], the stacking interactions of sparsomycin in a complex of H50S [5] are with the other side of A2602.

Compared with puromycin, sparsomycin is less useful for functional studies as it binds to the center of the PTC and triggers significant conformational alterations in both the A- and the P-sites [8], which, in turn, influence the positioning of both the A- and P-site tRNAs and may enhance nonproductive tRNA binding. The influence of sparsomycin on the A-site conformation contributes, most probably, to its inhibitory effect. Thus, although sparsomycin does not competitively inhibit A-site substrate binding, it interferes with the binding of A-site antibiotics, like chloramphenicol, and mutations of A-site nucleotides increase the tolerance to sparsomycin [45,47].

A sizable two-fold symmetry-related region within asymmetric ribosome

We detected an approximate two-fold symmetry within the PTC of D50S (Figs 2 and 3), relating the backbone-fold and base-conformations, rather than base types, of two groups of about 90 nucleotides each, many of which are highly conserved. This region is positioned between the two lateral protuberances of the large ribosomal subunit. Most of the symmetry-related nucleotides could be superimposed on their related nucleotides with no apparent deviations, whereas the two-fold relations of others may differ slightly in conformation. This local symmetry is consistent with the two-fold symmetry that relates puromycin derivatives in the active site as well as the 3′ termini of the docked tRNA [1,3,5,6]. The motions of the tRNA molecules originating from this local symmetry explain why the 3′ ends of the A- and P-site tRNAs are related by a 180° rotation whereas their helical features are related by a shift [1,48,49].

The two-fold related region consists of three semicircular shells. The inner shell, which was detected first [8], contains the PTC nucleotides that interact directly with the 3′ termini of the bound or translocated tRNA molecules (Figs 2 and 3). These include about half a dozen central loop nucleotides, the parts of H89 and H93 that point into the core of the symmetry-related region (called here the 'inner strands') and the A- and the P-loops (that are the stem loops of helices H80 and H92). The second (middle) shell includes helices H80 and H92, the stems of the A- and the P-loops, H74 and H90. The outer shell includes the H89 and H93 nucleotides that base-pair with those belonging to the inner

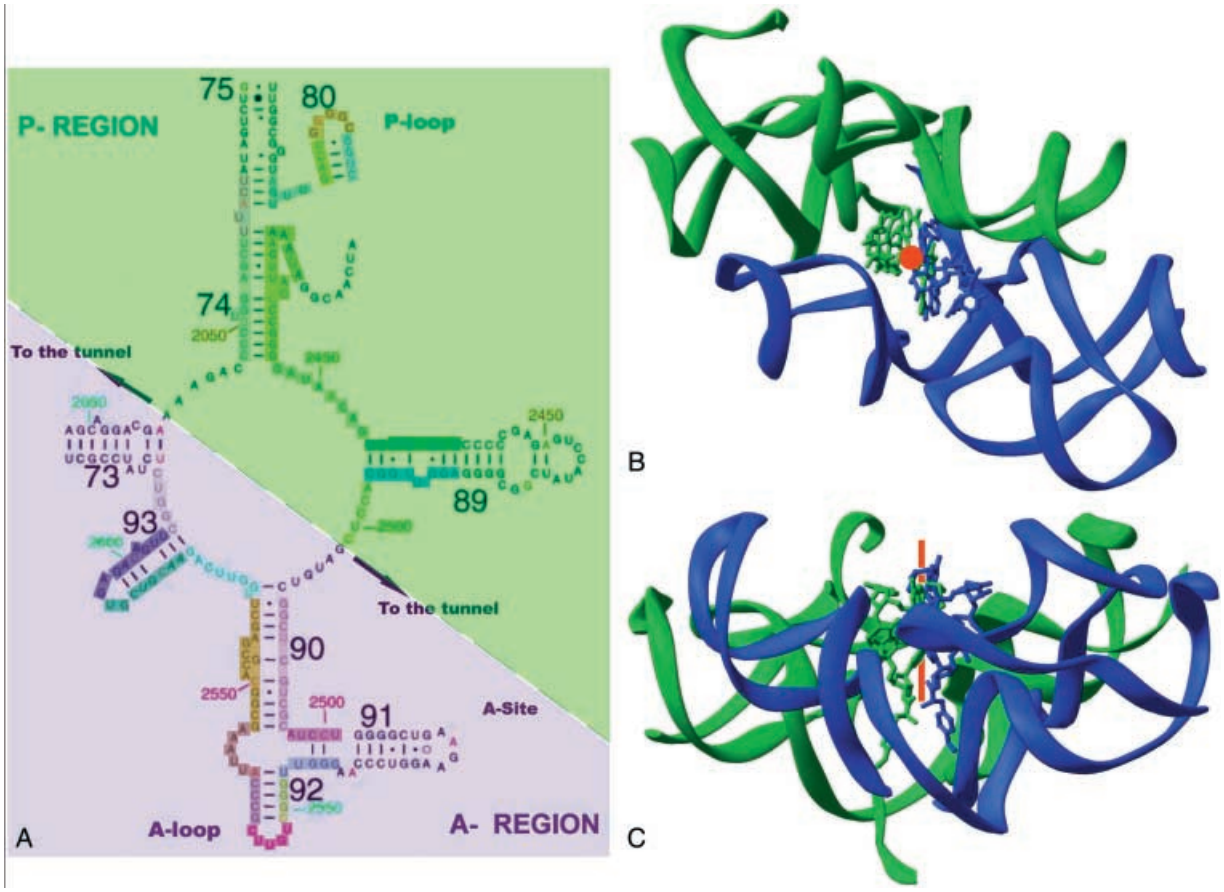

Fig. 2. The symmetry-related region. (A) Two-dimensional diagram of the 23S region of the PTC in D50S. The symmetry-related features are colored identically. The lower half of the figure can be correlated with the A-site region, and the upper side with the P-site region. *D. radiodurans* base numbering is shown in red, and *E. coli* in green. (B and C) Two views of the PTC. The symmetry-related RNA regions are shown as ribbons in blue and green, designated the features of the A- and the P-site regions, respectively. The same coloring scheme applies to the 3′ ends of ASM and of the rotated RM (shown as atoms). The cross-section and the parallel views of the two-fold symmetry axis are shown in red.

shell (called here the 'outer strands') and the parts of H75 and H91 that are positioned close to the other components obeying the two-fold symmetry. Detailed account of symmetry and deviation from it will be presented elsewhere (Agmon, A., unpublished results).

The detection of two-fold symmetry in all known structures of ribosomal large subunits [1–10] verified its universality and led us to reveal a two-fold rotation axis within the PTC. Initially the two-fold axis in the D50S PTC was observed visually within the nucleotide couples that interact with the 3′ tRNA termini and belong to the inner shell [8]. For the definition of the two-fold axis, a transformation matrix was first calculated for each of the symmetry-related nucleotide couples belonging to the inner shell, and then verified by calculating the global rotation axis, using all the components of the

Fig. 3. The A- to P-site rotating motion and peptide bond formation. (A) A projection down the two-fold rotation axis within the core of the symmetry-related region in D50S. The two-fold axis is marked by a black circle. The A-site features are shown in blue and the P-site in green, following the two-dimensional scheme in Fig. 2A. A2602 is colored in pink. (B) and (C) show several different orientations of A2602 in 50S complexes: ASM, a 35 nucleotide tRNA acceptor stem mimic [8]; SPAR, the complex of D50S with sparsomycin [8]; ASMS, D50S with ASM in the presence of sparsomycin [8]; and CAM, D50S with chloramphenicol. 1FG0 and 1KQS are the Protein Data Bank entries of complexes of H50S with two substrate analogs [3,6], docked onto D50S structure. The locations of the drugs sparsomycin and puromicyn are shown in gold and green, respectively. Snapshots of the spiral motion from the A-site (blue) to the P-site (green), obtained by successive rotations of the RM by 15° each around the two-fold axis, are shown in (B) and (D). This passage is represented by the transition from the A-site aminoacylated tRNA (in blue) to the P-site (in green). (D) Orthogonal views of tRNA-3′ end rotatory motion from A- to P-site. Top: views from the tunnel towards the PTC; bottom right: a view down the two-fold rotation axis. In both A73 was removed from the RM because of its proximity to the rotation axis. Bottom left: A stereo view perpendicular to the two-fold axis. The PTC backbone is shown in grey and the rear-wall nucleotides in red (top and bottom right) or grey (bottom left). The anchoring nucleotides, A2602 and U2585, are shown in magenta and pink, respectively. The blue-green round arrows indicate the rotation direction.

symmetry-related region. The rotation axes computed for the symmetry-related regions of all of the structures determined by us [7–10] show negligible variability, thus validating the existence and the definition of the symmetry-related region. Interestingly, among the nucleotide couples belonging to the inner shell and contacting the lower part of the 3′ termini of the tRNA molecules, four of the P-site nucleotides are located somewhat deeper in the PTC, compared with their mates at the A-site. Consequently, for this region the transformation matrix has a spiral nature, as it possesses a small translation towards the tunnel. These nucleotides are positioned at the entrance to the exit tunnel, and their orientation implies that they may guarantee the entrance of the nascent chain into it [8].

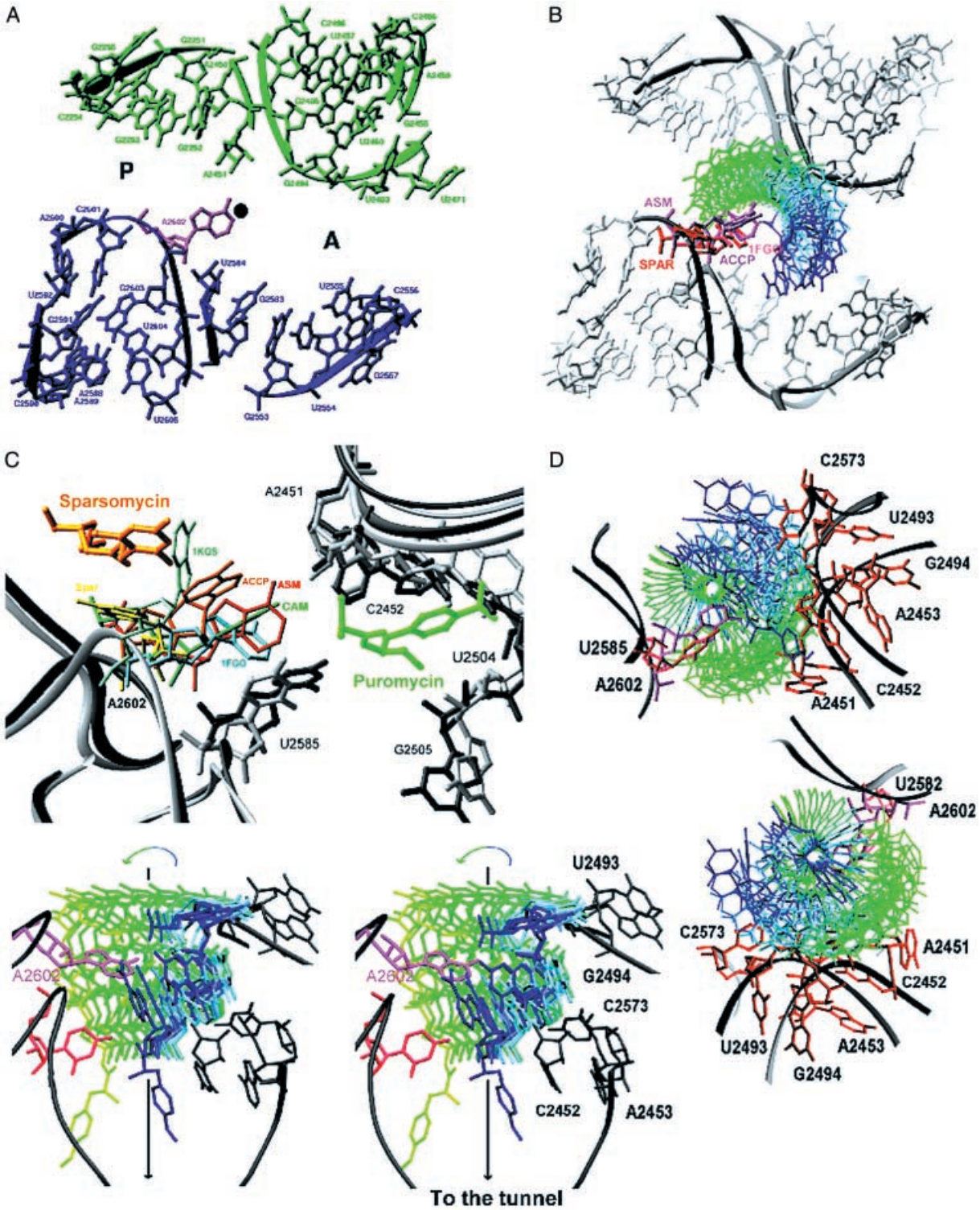

The deviations from perfect two-fold symmetry vary between nucleotide-couples. For example, the nucleotides located at the edges of the A- and P-loops, 2556–7 and 2254–5, respectively, can be superimposed on each other with no apparent deviations, whereas noticeable differences are found between their neighbors, 2554–5 and 2252–3. The first nucleotide group interacts with C74 of the A-site tRNA, namely the tRNA mimic ASM [8], or the docked tRNA molecule, and its mate with the docked P-site tRNA. These nucleotides also interact with the corresponding moieties of the puromycin derivatives that were bound to H50S, despite the differences between the PTC structure in H50S vs. D50S [7] and although some of the H50S PTC nucleotides undergo conformational alterations upon substrate analogs binding [3]. Importantly, G2250, which bulges out from the P-loop and interacts with the flexible loop of protein L16, deviates significantly from the two-fold symmetry, presumably in order to stabilize the conformation favorable for the remote interactions of this protein with the A-site tRNA. These interactions were found to provide a significant portion of the template for correct positioning of the A-site tRNA [8], indicating a possible interplay between the P- and the A-sites within the PTC.

The rotatory motion of the tRNA termini

Next, we questioned why the 3′ ends of the A- and P-site tRNAs are related by a local two-fold axis, whereas the helical features seem to translocate by a shift. The observation of a universal symmetry-related region within the active site of the ribosome, a particle that appears to lack any other internal symmetry, and the high sequence conservation of the inner PTC nucleotides, hint at a central functional relevance. Analysis of the properties of this region illuminated a unified mechanism for the formation of the peptide bond, the translocation of the tRNA molecules and the entrance of nascent proteins into the exit tunnel. According to this mechanism the passage of tRNA from the A- to the P-site involves two independent motions: a spiral rotation of $\approx 180°$ of the 3′ end of the A-site tRNA, performed in conjunction with peptide bond formation, and the shift of the acceptor stems of the tRNA. Sovereign motions of structural features of the tRNA, although of a different nature, were suggested previously and are the basis for the hybrid-state translocation mechanism [3,13].

The chemical bond between the phosphate and O3′ connecting the single stranded 3′ end of ASM and its double helical acceptor stem, which correspond to the bond connecting bases 72 and 73 of A-site tRNA, nearly overlaps with the two-fold axis. Accordingly, the entire single strand 3′ end, namely tRNA 73–76, was defined as the rotating moiety (called here RM). To validate the rotation motion we simulated the rotation of the RM of ASM around the two-fold axis and found that this motion could be performed with no spatial constraints or steric hindrance, and that throughout the rotation no conformational adjustments were required. Interestingly, the 5.5 Å crystal structure of the tRNA complexed T70S [1] suggests that tRNA-A73 is translated from A- to P-site together with tRNA acceptor stem. This implies that the rotated moiety is likely to be C74-A76 rather than A73-A76. A rotation of A73-A76 is compatible with our suggested motion, but the shorter rotating moiety will not be anchored to A2602.

Consistent with the requirement that the PTC must host both the A- and the P-site tRNA-3′ ends while peptide bond is being formed, we observed that the environment of the derived ASM-P-site 3′ end is similar to that of ASM. Furthermore, the derived P-site 3′ end of the tRNA mimic is positioned in a manner consistent with most of the available biochemical data [50], specifically, the A-site base-pair shared by all known structures, between C75 of A-site tRNA and G2553 [41], can be formed in the symmetry-related region. While rotating, the RM interacts with the rear-wall bases belonging to nucleotides C2573, A2451, and C2452, and slides along the backbone of G2494 and C2493 (Fig. 3). The RM interacts also with two nucleotides of the PTC front-wall. One of them is the flexible A2602, whose N1 atom is located in close proximity to the two-fold axis, and was found to be within contact distance with the rotating tRNA-A73 throughout the rotation. The second, U2585, is located between A2602 and the tunnel entrance, with its O4 close to the two-fold axis and its base interacting with the rotated A76.

A2602 was found to undergo a substantial conformational rearrangement upon the binding of each of the substrate analogs studied so far. As a consequence, it has a different orientation in each of the known structures of large subunit complexes. Combining the structures reported here and in [3,5,6,8] we demonstrated that A2602 can undergo a flip of $\approx 180°$ (Fig. 3). In all of the known complexes, A2602 is located within the space limited by two extreme conformations, the conformation induced by sparsomycin [8] and that observed in D50S complex with chloramphenicol [9]. A2602 is the only nucleotide in the PTC that displays such striking diversity. This great variability suggests that A2602 plays a dynamic role in the A- to P-site passage within the PTC, perhaps as a conformational switch that is likely to act in concert with H69, the other likely to be a conformational switch, assisting translocation near the subunit interface [7,8].

We found that the space available for A2602 throughout the rotatory motion of the tRNA molecule can accommodate all of its various conformations. Hence it seems that it functions as a molecular-propeller for the A $\rightarrow$ P passage of the tRNA-3′ end, and it is conceivable that the conformational changes of A2602 are synchronized with the RM rotation towards the P-site [8]. This mode of operation is consistent with the observed critical role of A2602 in the release of the nascent peptide during translation termination, when there is no A-site tRNA to replace the P-site tRNA [51]. Interestingly, A2602 is disordered in the H50S structure [2,3], but not in native D50S [7], similar to most functionally relevant features that are disordered in H50S.

Based on the conformation of the PTC front and rear-wall nucleotides, we conclude that the rear wall forms a scaffold that guides the motion from the A- to the P-site (Fig. 3). This guidance, together with the front-side anchoring, provides the precise path for the rotating moiety. Most of the rear-wall nucleotides are highly conserved, consistent with the universal nature of the tRNA A- to P-site passage. This requirement is somewhat released when the participation of the phosphate, rather than the base is required, as is the case of G2494, a rear-wall moiety that is less conserved.

This nucleotide is placed within the rear-wall, intruding between the rotating C74 and C75, and is stabilized by an adjacent A-minor motif (with H39) and the noncanonical base pair with U2457.

The differences in the distances between the RM and the rear- and front-walls could be correlated with their special tasks. The rear-wall directs the motion of the RM, and may interact with it. The two flexible nucleotides of the front wall, U2585 and A2602, seem to anchor the rotating moiety and undergo conformational rearrangements that may be coupled with the RM motion (Fig. 3). Hence the backbone of the front wall is positioned at a relatively large distance from the RM. Additional evidence for the rear-wall guidance was obtained from subsequent experiments, in which we allowed deviations from rigidity of the RM, consistent with the known flexibility of tRNA-3′ ends. In these exercises, we found that the guidance of the rear-wall nucleotides together with the front-anchoring nucleotides restrict the possible motions of the RM nucleotides and limit their flexibility.

The formation of the peptide bond

The most significant biological implication of the two-fold rotation of the tRNA-3′ end is the resulting geometry that should lead to peptide bond formation (Fig. 4). Thus, the guidance of the RM motion by the PTC nucleotides leads to a mutual orientation of the tRNAs' 3′ ends, suitable for a nucleophilic attack of the A-site primary amine on the P-site tRNA carbonyl-carbon. Such attack should readily occur at the pH of D50S crystals (pH ≈ 7.8), which is also the optimal pH for functional activity of ribosomes from various sources, including *E. coli* and *H. marismortui* [13,19,22,33,40,52]. The orientation of the two substrates

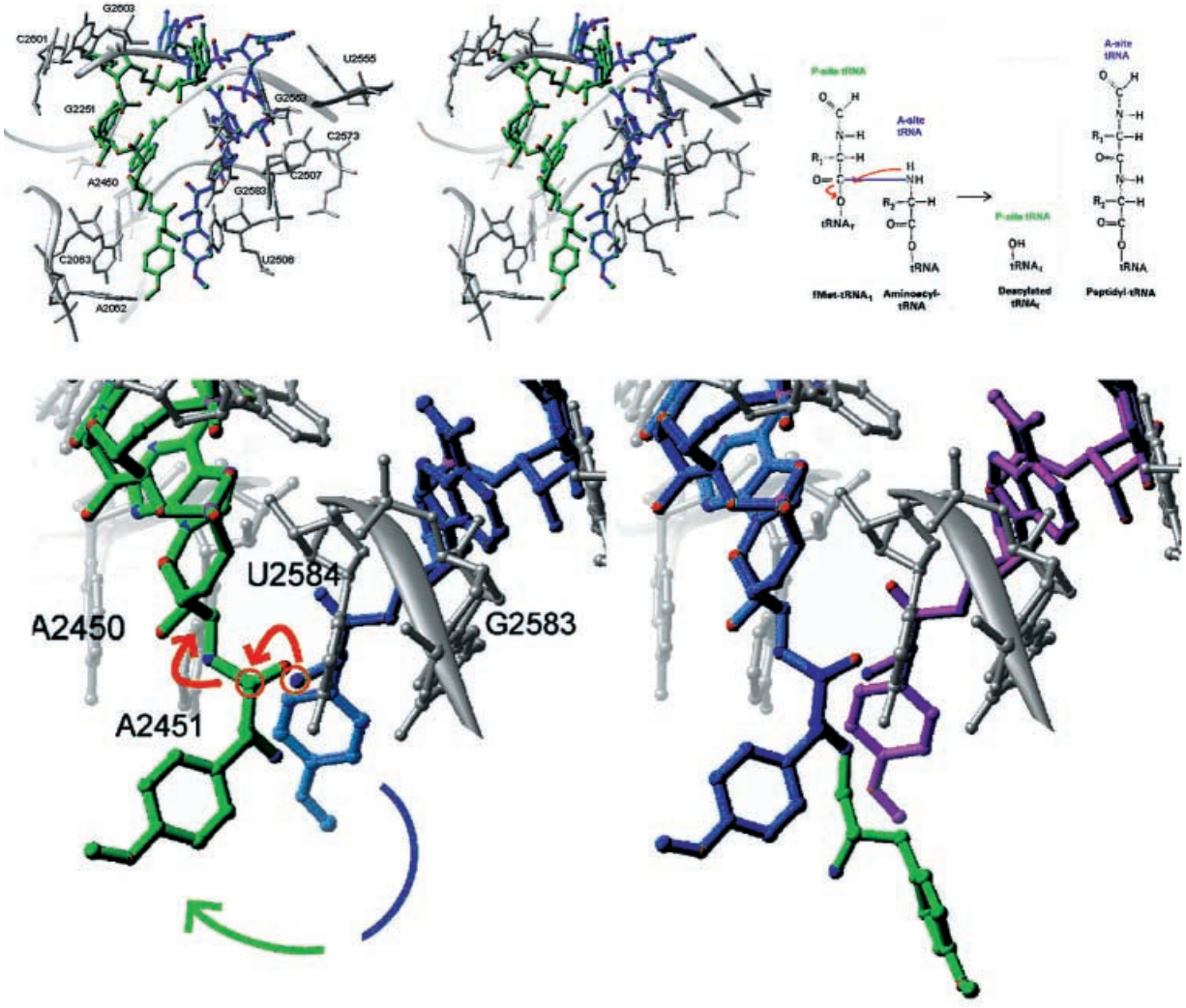

Fig. 4. Peptide bond formation. Top: (Left) A stereo view of the neighborhood of the peptidyl transferase center. ASM is shown in the A-site in blue and as the derived P-site, in green. (Right) The chemical formulation of peptide bond formation. Bottom: Our proposed mechanism for peptide bond formation. Left: The 3′ end of ASM (in blue) and the derived P-site tRNA in green. The small red arrows represent the transfer of a hydrogen during peptide bond formation. The red circles designate the nucleophilic amine (on the right) and the center of the oxyanion (on the left). Right: The reaction is completed. The nascent dipeptide (blue-green) points from the P-site into the tunnel. A new aminoacylated tRNA (violet) occupies the A-site.

and the distance between them allows the aminolysis of the ester bond, and the formation a tetrahedral oxyanion intermediate. The surrounding solvent may mediate the transfer of a hydrogen atom from the A-site tRNA α-amino group to the P-site tRNA leaving group. Release of the P-site tRNA, the leaving group, may be assisted by the flipping of the A-site 3′ end into the P-site, and by the reorganization of the attacked electrophile from sp^3 to sp^2 hybridization. Our proposed mechanism for peptide bond formation is consistent with results of footprinting experiments performed with 70S ribosome and tRNA molecules, showing that the A-tRNA acceptor stem end moves spontaneously into the P-site subsequent to peptide bond formation [13,31]. It supports the earlier biochemistry-based proposals that the catalytic activity of the ribosome is the provision of a template for accurate positioning and alignment of the tRNA molecules [13,24,27,31] rather then a direct participation in the chemical aspects of the enzymatic process, as suggested based on the structures of H50S complexes [3].

It remains to be seen whether the oxyanion intermediate needs stabilization. This can be obtained by the various components in the vicinity. In case stabilization is not required, the spontaneous formation of the peptide bond may also be autonomous. PTC components may assist the reaction by accelerating its rate. For cell vitality, rapid production of proteins may be required. This may explain the *in vitro* tolerance to the mutations of the PTC nucleotide A2541, which are known to be fatal *in vivo* [29,33,35].

In comparison with all steps of protein biosynthesis, excluding the GTPase hydrolysis, peptide bond formation has been characterized as a 'fast reaction' [53]. The rate of this irreversible step may be enhanced by ribosomal components, and the two-fold symmetry, serving as a degenerate template, seems to have a major dynamic role in the correct directionality of the entire protein biosynthesis process. Thus, once the incoming tRNA has been positioned in the PTC in its precise conformation, dictated by the PTC geometry, no additional rearrangements should be needed: The rotation of this tRNA, directed by two-fold symmetry components, carries it into the second part of the symmetrical template. Economizing on reorganization time is crucial for faster reaction rates, pushing the equilibrium of the chemical reaction to proceed towards peptide bond formation.

The A- to P-site rotation appears to be synchronized with peptide bond formation, or triggered by it. Furthermore, replacing the P-site tRNA-3′ end by the rotating moiety should facilitate the release of the leaving group. Translocation of the acceptor stems of both tRNA follows, freeing the space needed for binding of the next aminoacyl tRNA (Fig. 4) so that the following synthetic cycle can take place. Thus, besides facilitating peptide bond formation, an additional biological implication of the suggested motion is the provision for a smooth and efficient replacement of the P-site RM by the A-site. The sole geometrical requirement for our proposed mechanism is that the 3′ end of the P-site tRNA in the initiation complex has a conformation related to that of A-site by an approximate two-fold rotation.

Application of the two-fold rotation to all of the short A-site tRNA mimics studied so far [5,6,8], to an acceptor stem mimic not held in place by remote interactions due to the disorder of the features that should provide these interactions [3] or to an A-site tRNA acceptor stem mimic in the presence of an inhibitor [8], led to orientations less suitable for peptide bond formation. Such substrate analogs can form a single peptide bond, but unless accompanied by A- to P-site passage, no further protein biosynthesis can take place. An example is the fragment assay performed within H50S crystals. This reaction led to an A-site bound product, CCA-puromycin-phenylalanine-caproic acid–biotin, which was not passed to the P-site [6], either due to the low affinity of puromycin products to the P-site [5,6] and/or because the initial binding geometry of the puromycin derivative was not suitable for the specific rotating moiety rear-wall interactions.

The two-fold related region interacts with the two ribosomal protuberances

The question as to why the structure of the ribosome that lacks any symmetry possesses a region of about 180 nucleotides that obey a two-fold symmetry is only partially answered by the need for two similar environments at the binding sites of the 3′ end termini of the A- and P-site tRNA molecules, as only about a dozen nucleotides create these environments.

The two-fold symmetry-related region extends between the two lateral protuberances of the large ribosomal subunit. It connects the stems of the L1 (H76-H78 and protein L1) and the L7/L12 stalks (H43-H44, the loop of H95, called also the sarcin-ricin site, and proteins L10, L11 and L12). H76-H78 are directly connected to H75, and, from the opposite side, helix H91 reaches the sarcin-ricin loop and the part of helix H89 that does not obey the two-fold symmetry, interacts with H43-H44. Both features are involved in functional activities of the ribosome. Like most of the functionally relevant features, these two arms are disordered in the structure of H50S [2], whereas in the unbound D50S they are clearly resolved [7], presumably because this structure was determined under conditions close to physiological. The L7/L12 stalk, together with protein L11 and the sarcin-ricin loop, is involved in the contacts with the translocational factors, in factor-dependent GTPase [54], in elongation factor activities [55], and in the entrance of the aatRNA into the functioning ribosome.

The L1 stalk is facilitating the release of the E-site tRNA molecules. In accord with biochemical experiments [56], being extremely flexible, it adopts a different conformation in each of the structures of the large subunit [1,2,7] or of its components [57] known to date. In the complex of T70S with three tRNA molecules, the L1 stalk interacts with the elbow of E-tRNA and blocks the exit path for the E-tRNA [1]. In D50S, the L1 arm is placed further from its position in the T70S ribosome, in a position that would not interfere with the released of the exit (E)-site tRNA [7]. This motion corresponds to a $\approx 30°$ tilt around a local pivot which shares similar structural elements in both the bound and the unbound structures, and it is conceivable that the mobility of the L1 arm can be utilized for facilitating the release of E-site tRNA [7,15].

Analysis of the structure of the entire symmetry-related region suggests that each of its three shells has a specific

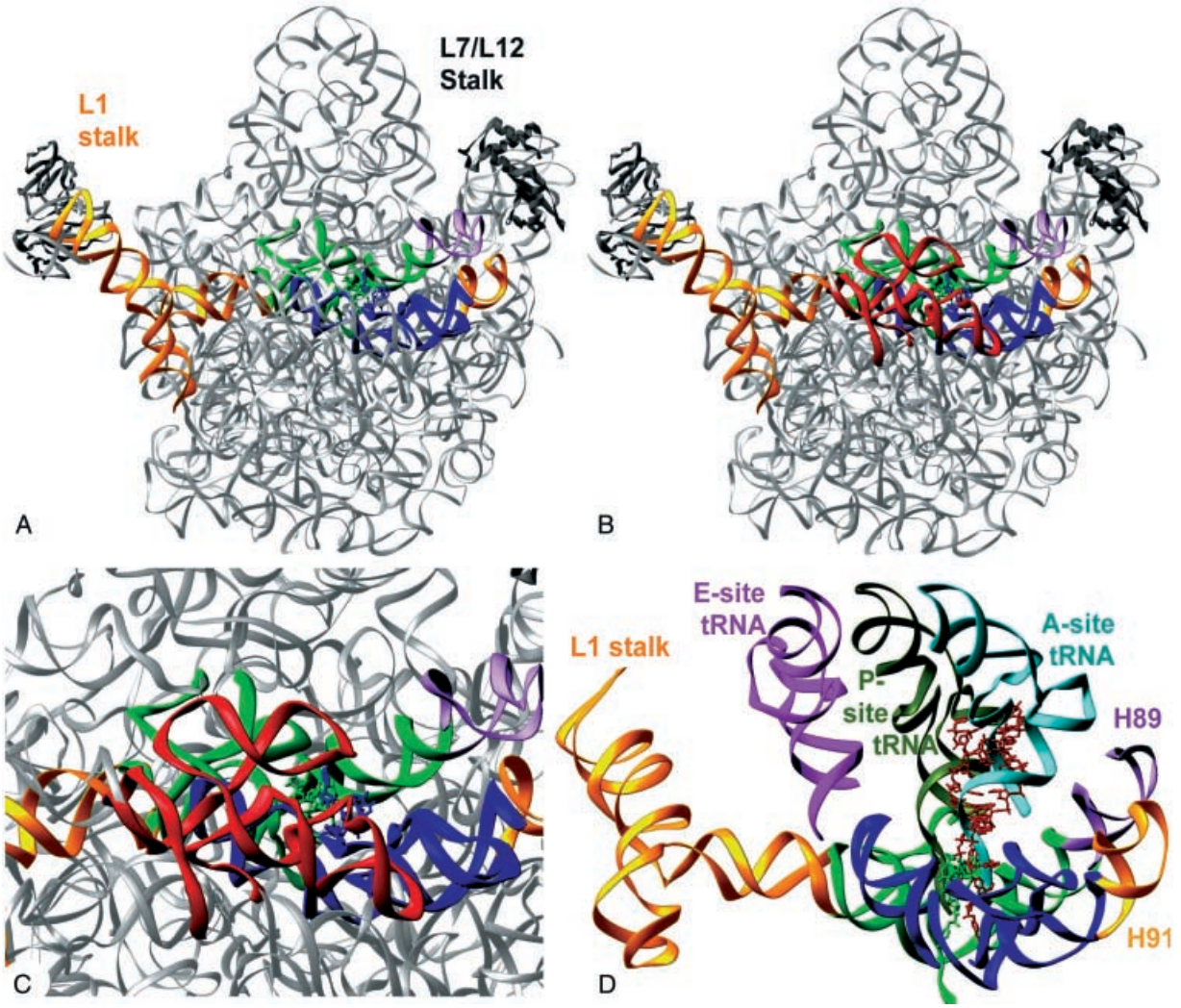

Fig. 5. The symmetry-related region and its contacts with the ribosomal stalks. (A and B) The location of the two-fold related region within D50S (represented by its RNA backbone in grey). Shown are the symmetry-related PTC features (in green and blue, as in Fig. 3), and their direct extensions (in gold and pink): H75-H79 that reach the E-tRNA gate, the L1 (in gold, connected to the green feature on the left); H89 extension (in dark pink, on the right) that interacts with L7/L12 stalk (the GTPase center); and H91 extension, which interacts with the sarcin-ricin loop, is shown in gold (connected to the blue feature, on the right). In (B) the H69 intersubunit bridge, which connects the PTC to the decoding center in the small subunit, and its extension, H70-H71, are colored red. Their location hints at their potential role in transmitting signals between the two lateral protuberances of the large subunit and the small one. (C) Focus on the central part of the view shown in (B). (D) The symmetry-related region together with ASM (red), the rotated RM (green, shown as atoms) and the docked A-, P- and E-site tRNAs (in cyan, green and pink, respectively).

task. The inner shell appears to provide symmetrical environments within the PTC for both the A- and the P-site tRNA, consistent with requirement to host both termini while the peptide bond is being formed (Fig. 5). H74 and H90 of the middle shell are the long helical features that connect between the sequence-distant P- and A-loops of the inner shell (via H80 and H92), respectively, thus maintaining the symmetrical requirements of the PTC. It seems therefore that increasing the stability of the PTC core structure is the task of the second shell of the symmetry-related region.

Transmission of signals between ribosomal features that are involved in the entire process of protein biosynthesis can also be associated with the symmetry-related region. Features radiating from the outer shell of the symmetry-related region interact with the L1 and the L7/L12 stalks (Fig. 5). It is therefore conceivable that the outer shell of the symmetry-related region plays a role in the transmission of signals between the ribosomal features facilitating the two ends of the biosynthetic process: the entry of the amino acylated tRNA that is about to participate in peptide bond formation, and the release of the free E-site tRNA, after the formation of the peptide bond.

Gating the ribosomal tunnel

Once produced, the nascent proteins emerge out of ribosomes through a tunnel adjacent to the PTC. Four nucleotides of the P-site guarantee the entrance of the nascent protein into the exit tunnel, by forming a configuration suitable for this task. This exit tunnel, first observed in

mid-1980s [58,59], was assumed to provide a passive path for protein export and was described as having a 'non sticky' nature [3]. However, the progression of the nascent chain through the tunnel is far from smooth, as the walls of the exit tunnel have bumps and grooves and its diameter is not uniform.

This tunnel is the target of macrolide antibiotics. Macrolides, as well as the more advanced compounds derived from them, namely azalides and ketolides, are built of a lactone ring (of 14–16 members) and one or two sugar moieties and interfere with protein biosynthesis by blocking the tunnel near its entrance (Fig. 6) [4,9,10,60,61].

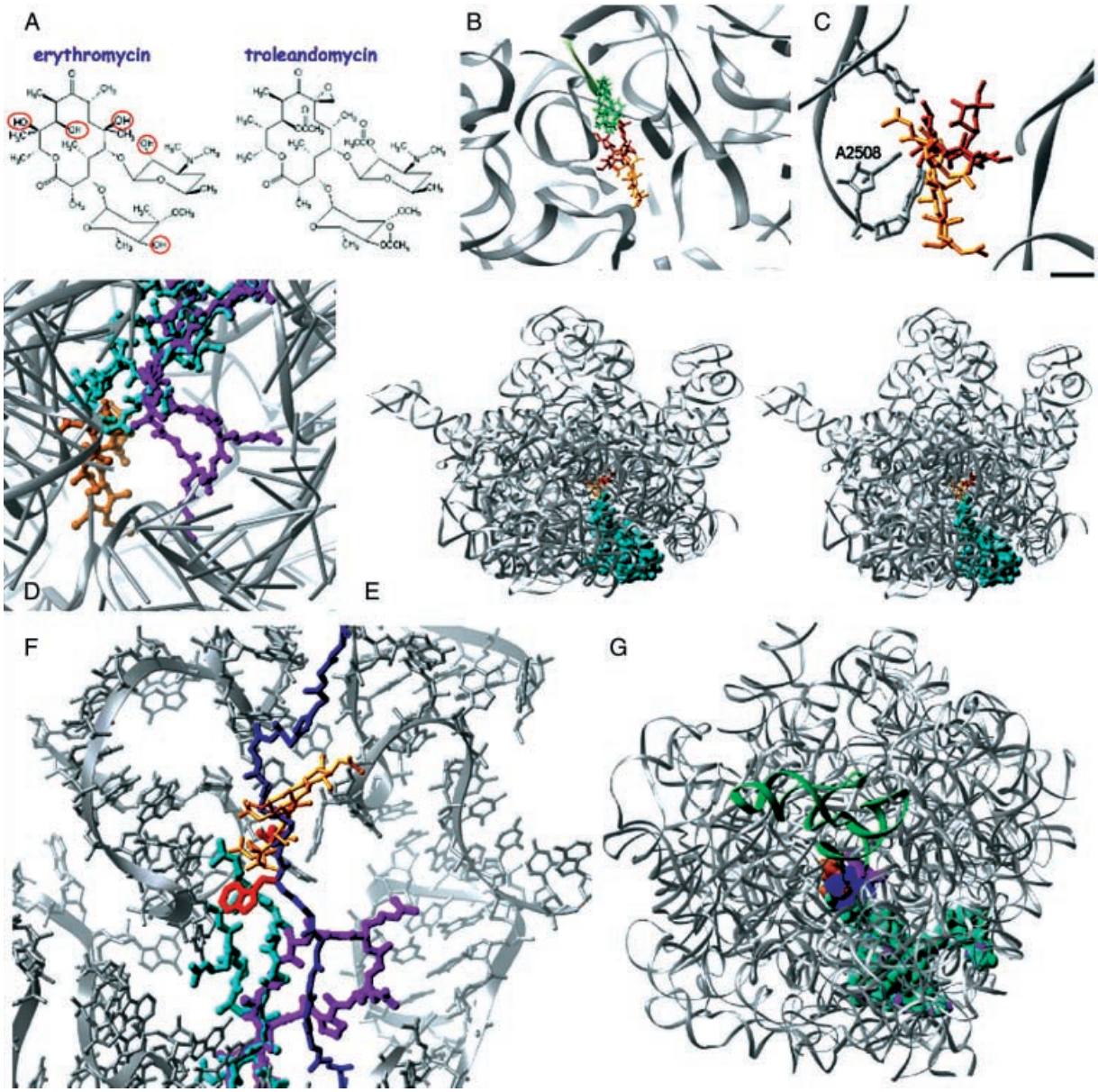

Fig. 6. Gating of the ribosomal tunnel by the tip of L22 β-hairpin. In all: D50S RNA is shown as grey ribbons. The tip of the β-hairpin of protein L22 at its native conformation is shown in cyan, and the swung conformation in magenta. TAO is shown in gold and erythromycin in red. (A) The chemical formulae of erythromycin and TAO, highlighting the hydroxyls that do not exist in TAO. (B) View along the tunnel, shown the positions of erythromycin and TAO. A modeled five-residue peptide is shown in light green. The tip of the 3′ end of P-site tRNA is shown in olive-green. (C) A closer view of (B) focusing on the binding modes of TAO and erythromycin and highlighting the ribosome pocket with which the macrolides form the most extensive contacts. (D) A view into the tunnel from the PTC, showing the positions of L22 hairpin tip in its native and swung conformations, together with TAO. (E) A stereo view of the backbone of the entire RNA (grey) of D50S and protein L22, which is shown as a space filled model. Also shown are Erythromycin and TAO. (F) Side view of the upper region of the tunnel, showing TAO binding site and the native and the swung conformations of L22 β-hairpin tip. A modeled poly(Ala) nascent chain is shown in blue with the positions of the crucial Trp and Ile in red. (G) A view into the tunnel from the PTC of D50S. The native and the swung conformations and TAO, as well as TAO and the modeled nascent chain (as in F) are shown as space filled models. P-site tRNA is shown as a green ribbon.

All 14-member ring macrolides studied so far make intensive contacts with A2058 of the 23S RNA of eubacterial large ribosomal subunit [9,10,60,61], consistent with various biochemical results, reviewed in [62]. A2058 was implicated in macrolide resistance, which is often acquired by the addition of bulky substituents to it either by mutation to guanine, or by the methylation of the adenine by Erm methylases [62,63]. Consistently, the selectivities of 14-membered ring macrolides are dictated by the base in position 2058; in contrast to eubacteria where adenine is commonly found in this position, eukaryotes and archaea possess guanine. However, bacteria with guanine in position 2058 are somewhat less selective for the binding of 15- or 16-ring macrolides. It was found that the binding mode of 15-ring macrolides to ribosomes with guanine in position 2058 is different to that observed for binding to eubacteria with A in position 2058, and causes less severe tunnel blockage [10]. Furthermore, the binding of the 15- and 16-member ring macrolides to ribosomes with G in position 2058, as is the case of the archaeon *H. marismortui* [4], requires significantly higher concentrations than those used clinically. Hence, in this critical aspect, *H. marismortui* resembles eukaryotes more than prokaryotes.

Troleandomycin (TAO) is a macrolide that besides hampering protein biosynthesis, inactivates the liver cytochrome P450 metabolite complexes, and hence is less useful clinically [64]. This semisynthetic macrolide is structurally similar to erythromycin (Fig. 6) but has an oxirane ring instead of the methyl of the lactone ring. Furthermore, in TAO all erythromycin hydroxyl groups are either methylated or acetylated [65]. We found that TAO is located somewhat deeper in the tunnel with its lactone ring is almost parallel to the tunnel wall [60], instead of being nearly perpendicular, as is the case for erythromycin binding (Fig. 5). We attributed this binding mode to the inability of TAO to create the hydrogen bonds typical of macrolides as well as to the bulkiness of its substituents.

Apart from unique interactions with protein L32 and with helices H35 and H35a, TAO introduces striking conformational rearrangements in the exit tunnel [60] by flipping the tip of the β-hairpin of protein L22 (Fig. 6). Protein L22 consists of a single globular domain and a highly conserved β-hairpin with a unique twisted conformation [66]. Within the ribosome, it is positioned with its globular domain on the surface of the large ribosomal subunit at the tunnel opening; its β-hairpin lines the exit tunnel wall (Fig. 6) and its overall conformation is similar to that seen in its own crystal structure, except for a small difference in the inclination of the tip of the β-hairpin [3,7]. This β-hairpin maintains its length in all species, whereas insertions as well as deletions exist in other regions of L22.

The tip of the β-hairpin of L22 is built of 11 residues and contains a short loop built of two highly conserved positively charged amino acids (arginines or lysines). This short loop seems to act as a double-hook for interacting with the tunnel wall. In native D50S the side chains of the double hook are embedded in narrow grooves, and thus the space available for conformational rearrangements of the double hook are rather limited. In its complex with D50S, TAO occupies the space used by one of the arginines of the double hook, and this seems to trigger a swing across the tunnel of the entire tip of L22 β-hairpin, around an internal hinge region (Fig. 6). Both the native and the swung conformation of L22 β-hairpin are stabilized mainly by electrostatic interactions and hydrogen bonds with the backbone of rRNA [60].

The intrinsic conformational mobility of L22 hairpin tip and the existence of the highly conserved double-hook, capable of anchoring both the native and swung conformations, indicates that the structure of protein L22 β-hairpin has been designed for a gating role. The precise positioning of the hinge region, required for the accurate swinging motion and the resulting and anchoring across the tunnel, is presumably achieved by the pronounced positive surface charges of this region [66].

Elongation arrest

Evidence for tunnel participation in regulating intracellular cotranslational processes was recently reported for several eubacterial and eukaryotic systems. All of these studies indicated that the tunnel may respond to specific sequence motifs of nascent chains that can affect protein elongation in prokaryotes and in mammalian cells [67–71], and act as a discriminating gate. Striking examples are SecM, a protein belonging to the secretion monitoring system, which monitors protein export [72,73], and the nascent leader peptide of *E. coli* tryptophanase (tnaC) operon [74]. The SecM protein is produced in conjunction with a protein export system, and contains a 'pulling protein', which recognizes an export signal located at the protein N-terminus [72]. The amino acid sequence of SecM includes a sequence motif FXXXXWIXXXXGIRAGP that, in the absence of the protein export system, causes elongation arrest during translation of SecM in *E. coli*. This particular sequence motif was also found to hinder translation elongation in *E. coli* when present in the unrelated sequence of LacZ-alpha protein [72], indicating that the elongation arrest is independent of the sequence context. Mutations in the 23S ribosomal RNA in the vicinity of the double hook binding or in the β-hairpin of protein L22 were shown to bypass the elongation arrest [72].

The swing of protein L22 hairpin tip could be linked to the putative regulatory role assigned to the tunnel. We base this linkage on the severe restriction of the space available for the passage of nascent proteins through the tunnel by the swung conformation of L22; on the conservation of the L22 double-hook; and on the finding that sequence related translational arrest could be suppressed by mutations localized in the L22 double-hook region [72]. We propose that L22 is a main player in this task, with its double-hook acting as a conformational switch and providing the molecular tool for the gating and the discriminative properties of the ribosome tunnel. In support of our proposal are the arrest-suppressing mutations of L22, namely Gly91 → Ser, Ala93 → Thr, and Ala93 → Val, all of which introduce bulkier residues that should destabilize the swung conformation. The deletion of Met82EC-Lys-Arg in L22, also known to confer erythromycin resistance, induces arrest-alleviation, and it was investigated by superposing the structure of this mutant [75] onto D50S structure. This deletion shortens the L22 β-hairpin and displaces the hinge region, compared with its position in native D50S. Such displacement does not severely affect

the extensive network of interactions of L22 hairpin with the tunnel wall in the native structure, whereas it may alter the swing motion and prevent the formation of the swung double-hook stabilizing interactions with the opposite side of the tunnel. Analysis of the structure of this mutant showed that this deletion could affect the conformation of the nucleotides participating in erythromycin binding [75], in line with cryo-EM studies [76] and confirming our proposal that erythromycin resistance is due to indirect effects [9]. Further support for the linkage between the L22 swing and the arrest mechanism is the finding that suppression mutations of rRNA occur close to the location of L22 β-hairpin, thus may affect its positioning and consequently its conformation.

Within the sequence motif that was shown to induce elongation arrest in *E. coli* while SecM protein is being formed [72], the residues proline, tryptophan and isoleucine were identified to be the arrest triggers. A similar motif causes arrest the biosynthesis of the leader peptide of *E. coli* tryptophanase (tnaC) operon [74]. In both cases the combination of tryptophane and the proline and the spacing between then (a tryptophane located about 12 residues upstream from a proline), causes the elongation arrest.

In order to investigate the structural basis for the arrest mechanism we modeled a nascent chain of polyalanine within the exit tunnel, following its curvature [60]. We observed that once this proline has reached the tunnel entrance, i.e. it has been incorporated into the nascent chain; the crucial tryptophane reaches the tip of L22 β-hairpin a location close to that occupied by TAO (Fig. 6) and in [60]. Motions of the nascent chain could, in principle, allow the displacement of the tryptophane to the tunnel space available on the opposite side of the tunnel, as seems to happen for nascent chains containing tryptophane. However, the rigidity of the proline, which has just been incorporated into the nascent chain and is positioned at a very narrow tunnel region, should restrict the conformational space of the growing chain. Consequently, the motions of the entire chain required for progression of the nascent chain within the tunnel, should be minimized, and the collision between the tryptophane and the L22 double hook should trigger the swing of the entire β-hairpin tip, in a manner similar to that caused by TAO binding. As a result of the swinging, the space for the bulky side chains becomes free, but at the same time the progression of the nascent chain is jammed.

The mechanism whereby cellular signaling for arrest alleviation is transmitted to the ribosome and how the swinging back of L22 β-hairpin tip to its native conformation can be triggered remain to be explored. Importantly, elongation arrest occurs only in the absence of active export of SecM, whereas under normal cellular conditions this arrest was found to be transient [72]. We suggest that the L22 β-strand extension of its β-hairpin, which extends all the way to its C-terminus and is positioned at the vicinity of the exit tunnel opening, may be triggered by the 'pulling protein' and transmits such signals. The nascent chain may also play a role in the suppression of the elongation arrest, as in all systems studied so far the arrest motif is located in a position that when its proline reaches the PTC the N-terminus of the nascent chain has already emerged out of the exit tunnel, thus may interact with the 'pulling protein'. This suggestion is consistent with the finding that in SecM protein, this N-terminus region contains the export signaling sequence [72] and that nascent chains from inside the ribosome can induce structural alterations in of the translocon pore that line up directly with the exit tunnel [67].

Conclusions

We showed that remote directionality is the main factor for correct positioning of the tRNA in the PTC, and that precisely positioned tRNA analogs allow a spiral rotation of their 3′ end from the A- to the P-site around an axis identified by us within the ribosomal PTC. Based on the conformation of the PTC components that interact with the rotating moiety, we conclude that the PTC rear-wall forms a scaffold that in cooperation with the front-side nucleotides, guide the rotating moiety and provide the precise path that leads to an orientation suitable for peptide bond formation. The spiral rotation ensures the entrance of the nascent proteins into their exit tunnel, and it is likely that signal transmission between the incoming aminoacylated tRNA and the release of the free tRNA molecules is mediated by the symmetry-related region.

The identification of a two-fold symmetry in all known structures of the large subunit, the significant conservation of the nucleotides belonging to the inner symmetry-related region, and the resulting mutual orientation of A- and P-site tRNAs, suitable for peptide bond formation, are consistent with the universality of our proposed mechanism.

Our results also show that protein L22 that lines the nascent protein exit tunnel wall has an intrinsic conformational mobility and provides a double-hook, located at the tip of its long β-hairpin, which is capable of interacting with two sides of the tunnel wall. This flipping motion across the ribosomal tunnel may control the elongation of nascent chains. The common sequence dependence of the elongation arrest, the existence of arrest-suppression mutations that should affect L22 conformation, and the tunnel gating abilities indicate that the ribosome may be involved in cellular regulation processes.

Acknowledgements

Thanks are due to J. M. Lehn, M. Lahav and A. Mankin for critical discussions, and to R. Albrecht, W. S. Bennett, H. Burmeister, C. Glotz, C. Liebe, M. Laschever, C. Stamer, S. Meyer and A. Wolff for contributing to this work. These studies could not be performed without the cooperation and assistance of the staff of station ID19 of the SBC at APS/ANL. The Max Planck Society, the US National Institute of Health (GM34360), the German Ministry for Science and Technology (BMBF Grant 05-641EA), and the Kimmelman Center for Macromolecular Assembly at the Weizmann Institute provided support. A. Y. holds the Hellen & Martin Kimmel Professorial Chair.

References

1. Yusupov, M.M., Yusupova, G.Z., Baucom, A., Lieberman, K., Earnest, T.N., Cate, J.H. & Noller, H.F. (2001) Crystal structure of the ribosome at 5.5 Å resolution. *Science* **292**, 883–896.

2. Ban, N., Nissen, P., Hansen, J., Moore, P.B. & Steitz, T.A. (2000) The complete atomic structure of the large ribosomal subunit at 2.4 Å resolution. *Science* **289**, 905–920.
3. Nissen, P., Hansen, J., Ban, N., Moore, P.B. & Steitz, T.A. (2000) The structural basis of ribosome activity in peptide bond synthesis. *Science* **289**, 920–930.
4. Hansen, J.L., Ippolito, J.A., Ban, N., Nissen, P., Moore, P.B. & Steitz, T.A. (2002) The structures of four macrolide antibiotics bound to the large ribosomal subunit. *Mol. Cell.* **10**, 117–128.
5. Hansen, J.L., Schmeing, T.M., Moore, P.B. & Steitz, T.A. (2002) Structural insights into peptide bond formation. *Proc. Natl Acad. Sci. USA* **99**, 11670–11675.
6. Schmeing, T.M., Seila, A.C., Hansen, J.L., Freeborn, B., Soukup, J.K., Scaringe, S.A., Strobel, S.A., Moore, P.B. & Steitz, T.A. (2002) A pre-translocational intermediate in protein synthesis observed in crystals of enzymatically active 50S subunits. *Nat. Struct. Biol.* **9**, 225–230.
7. Harms, J., Schluenzen, F., Zarivach, R., Bashan, A., Gat, S., Agmon, I., Bartels, H., Franceschi, F. & Yonath, A. (2001) High resolution structure of the large ribosomal subunit from a mesophilic eubacterium. *Cell* **107**, 679–688.
8. Bashan, A., Agmon, I., Zarivach, R., Schluenzen, F., Harms, J., Berisio, R., Bartels, H., Franceschi, F., Auerbach, T., Hansen, H.A.S., Kossoy, E., Kessler, M. & Yonath, A. (2003) Structural basis for a unified machinery of peptide bond formation, translocation and nascent chain progression. *Mol. Cell.* **11**, 91–102.
9. Schluenzen, F., Zarivach, R., Harms, J., Bashan, A., Tocilj, A., Albrecht, R., Yonath, A. & Franceschi, F. (2001) Structural basis for the interaction of antibiotics with the peptidyl transferase centre in eubacteria. *Nature* **413**, 814–821.
10. Schluenzen, F., Harms, J., Franceschi, F., Hansen, H.A.S., Bartels, H., Zarivach, R. & Yonath, A. (2003) Structural basis for the antibiotic activity of ketolides and azalides. *Structure* **11**, 329–338.
11. Lill, R. & Wintermeyer, W. (1987) Destabilization of codon–anticodon interaction in the ribosomal exit site. *J. Mol. Biol.* **196**, 137–148.
12. Rheinberger, H.J., Sternbach, H. & Nierhaus, K.H. (1981) Three tRNA binding sites on *Escherichia coli* ribosomes. *Proc. Natl Acad. Sci. USA* **78**, 5310–5314.
13. Moazed, D. & Noller, H.F. (1989) Intermediate states in the movement of transfer RNA in the ribosome. *Nature* **342**, 142–148.
14. Noller, H.F., Yusupov, M.M., Yusupova, G.Z., Baucom, A. & Cate, J.H. (2002) Translocation of tRNA during protein synthesis. *FEBS Lett.* **514**, 11–16.
15. Yonath, A. (2002) The search and its outcome: high-resolution structures of ribosomal particles from mesophilic, thermophilic, and halophilic bacteria at various functional states. *Annu. Rev. Biophys. Biomol. Struct.* **31**, 257–273.
16. Gale, E.F., Cundliffe, E., Reynolds, P.E., Richmond, M.H. & Waring, M.J. (1981) *The Molecular Basis of Antibiotic Action*. Wiley, London.
17. Green, R., Switzer, C. & Noller, H.F. (1998) Ribosome-catalyzed peptide-bond formation with an A-site substrate covalently linked to 23S ribosomal RNA. *Science* **280**, 286–289.
18. Moazed, D. & Noller, H.F. (1991) Sites of interaction of the CCA end of peptidyl-t-RNA with 23S rRna. *Proc. Natl Acad. Sci. USA* **88**, 3725–3728.
19. Noller, H.F., Hoffarth, V. & Zimniak, L. (1992) Unusual resistance of peptidyl transferase to protein extraction procedures. *Science* **256**, 1416–1419.
20. Odom, O.W., Picking, W.D. & Hardesty, B. (1990) Movement of tRNA but not the nascent peptide during peptide bond formation on ribosomes. *Biochemistry* **29**, 10734–10744.
21. Porse, B.T. & Garrett, R.A. (1995) Mapping important nucleotides in the peptidyl transferase centre of 23 S rRNA using a random mutagenesis approach. *J. Mol. Biol.* **249**, 1–10.
22. Rodriguez-Fonseca, C., Phan, H., Long, K.S., Porse, B.T., Kirillov, S.V., Amils, R. & Garrett, R.A. (2000) Puromycin–rRNA interaction sites at the peptidyl transferase center. *RNA* **6**, 744–754.
23. Vazquez, D. (1979) Inhibitors of protein biosynthesis. *Mol. Biol. Biochem. Biophys.* **30**, 1–312.
24. Cooperman, B.S. (1977) Identification of binding sites on the *E. coli* ribosome by affinity labeling. *Adv. Exp Med. Biol.* **86A**, 595–609.
25. Green, R. & Noller, H.F. (1997) Ribosomes and translation. *Annu. Rev. Biochem.* **66**, 679–716.
26. Krayevsky, A.A. & Kukhanova, M.K. (1979) The peptidyltransferase center of ribosomes. *Prog. Nucleic Acid Res. Mol. Biol.* **23**, 1–51.
27. Nierhaus, K.H., Schulze, H. & Cooperman, B.S. (1980) Molecular mechanisms of the ribosomal peptidyl transferase center. *Biochem. Int.* **1**, 185–192.
28. Pape, T., Wintermeyer, W. & Rodnina, M. (1999) Induced fit in initial selection and proofreading of aminoacyl-tRNA on the ribosome. *EMBO J.* **18**, 3800–3807.
29. Polacek, N., Gaynor, M., Yassin, A. & Mankin, A.S. (2001) Ribosomal peptidyl transferase can withstand mutations at the putative catalytic nucleotide. *Nature* **411**, 498–501.
30. Samaha, R.R., Green, R. & Noller, H.F. (1995) A base pair between tRNA and 23S rRNA in the peptidyl transferase centre of the ribosome. *Nature* **377**, 309–314.
31. Wilson, K.S. & Noller, H.F. (1998) Molecular movement inside the translational engine. *Cell* **92**, 337–349.
32. Barta, A., Dorner, S. & Polacek, N. (2001) Mechanism of ribosomal peptide bond formation. *Science* **291**, 203.
33. Bayfield, M.A., Dahlberg, A.E., Schulmeister, U., Dorner, S. & Barta, A. (2001) A conformational change in the ribosomal peptidyl transferase center upon active/inactive transition. *Proc. Natl Acad. Sci. USA* **98**, 10096–10101.
34. Parnell, K.M., Seila, A.C. & Strobel, S.A. (2002) Evidence against stabilization of the transition state oxyanion by a p*K*a-perturbed RNA base in the peptidyl transferase center. *Proc. Natl Acad. Sci. USA* **99**, 11658–11663.
35. Thompson, J., Kim, D.F., O'Connor, M., Lieberman, K.R., Bayfield, M.A., Gregory, S.T., Green, R., Noller, H.F. & Dahlberg, A.E. (2001) Analysis of mutations at residues A2451 and G2447 of 23S rRNA in the peptidyltransferase active site of the 50S ribosomal subunit. *Proc. Natl Acad. Sci. USA* **98**, 9002–9007.
36. Moore, P.B. & Steitz, T.A. (2003) After the ribosome structures: how does peptidyl transferase work? *RNA* **9**, 155–159.
37. Katunin, V.I., Muth, G.W., Strobel, S.A., Wintermeyer, W. & Rodnina, M.V. (2002) Important contribution to catalysis of peptide bond formation by a single ionizing group within the ribosome. *Mol. Cell.* **10**, 339–346.
38. White, O., Eisen, J.A., Heidelberg, J.F., Hickey, E.K., Peterson, J.D., Dodson, R.J., Haft, D.H., Gwinn, M.L., Nelson, W.C., Richardson, D.L., *et al.* (1999) Genome sequence of the radioresistant bacterium *Deinococcus radiodurans* R1. *Science* **286**, 1571–1577.
39. Levin-Zaidman, S., Englander, J., Shimoni, E., Sharma, A.K., Minton, K.W. & Minsky, A. (2003) Ringlike structure of the *Deinococcus radiodurans* genome: a key to radioresistance? *Science* **299**, 254–256.
40. Miskin, R., Zamir, A. & Elson, D. (1968) The inactivation and reactivation of ribosomal-peptidyl transferase of *E. coli*. *Biochem. Biophys. Res. Commun.* **33**, 551–557.
41. Kim, D.F. & Green, R. (1999) Base-pairing between 23S rRNA and tRNA in the ribosomal A site. *Mol. Cell.* **4**, 859–864.
42. Cundliffe, E. (1981) *Antibiotic Inhibitors of Ribosome Function*. Wiley, London, New York, Sydney, Toronto.

43. Goldberg, I.H. & Mitsugi, K. (1966) Sparsomycin, an inhibitor of aminoacyl transfer to polypeptide. *Biochem. Biophys. Res. Commun.* **23**, 453–459.
44. Porse, B.T., Kirillov, S.V., Awayez, M.J., Ottenheijm, H.C. & Garrett, R.A. (1999) Direct crosslinking of the antitumor antibiotic sparsomycin, and its derivatives, to A2602 in the peptidyl transferase center of 23S-like rRNA within ribosome-tRNA complexes. *Proc. Natl Acad. Sci. USA* **96**, 9003–9008.
45. Tan, G.T., DeBlasio, A. & Mankin, A.S. (1996) Mutations in the peptidyl transferase center of 23 S rRNA reveal the site of action of sparsomycin, a universal inhibitor of translation. *J. Mol. Biol.* **261**, 222–230.
46. Lazaro, E., van den Broek, L.A., San Felix, A., Ottenheijm, H.C. & Ballesta, J.P. (1991) Biochemical and kinetic characteristics of the interaction of the antitumor antibiotic sparsomycin with prokaryotic and eukaryotic ribosomes. *Biochemistry* **30**, 9642–9648.
47. Lazaro, E., Rodriguez-Fonseca, C., Porse, B., Urena, D., Garrett, R.A. & Ballesta, J.P. (1996) A sparsomycin-resistant mutant of *Halobacterium salinarium* lacks a modification at nucleotide U2603 in the peptidyl transferase centre of 23S rRNA. *J. Mol. Biol.* **261**, 231–238.
48. Agrawal, R.K., Heagle, A.B., Penczek, P., Grassucci, R.A. & Frank, J. (1999) EF-G-dependent GTP hydrolysis induces translocation accompanied by large conformational changes in the 70S ribosome. *Nat. Struct. Biol.* **6**, 643–647.
49. Stark, H., Orlova, E.V., Rinke-Appel, J., Junke, N., Mueller, F., Rodnina, M., Wintermeyer, W., Brimacombe, R. & van Heel, M. (1997) Arrangement of tRNAs in pre- and posttranslocational ribosomes revealed by electron cryomicroscopy. *Cell* **88**, 19–28.
50. Green, R. & Noller, H.F. (1999) Reconstitution of functional 50S ribosomes from *in vitro* transcripts of *Bacillus stearothermophilus* 23S rRNA. *Biochemistry* **38**, 1772–1779.
51. Polacek, N., Gomez, M.J., Ito, K., Xiong, L., Nakamura, Y. & Mankin, A. (2003) The critical role of the universally conserved A2602 of 23S ribosomal RNA in the release of the nascent peptide during translation termination. *Mol. Cell.* **11**, 103–112.
52. Shevack, A., Gewitz, H.S., Hennemann, B., Yonath, A. & Wittmann, H.G. (1985) Characterization and crystallization of ribosomal particles from *Halobacterium marismortui*. *FEBS Lett.* **184**, 68–71.
53. Rodnina, M.V. & Wintermeyer, W. (2001) Ribosome fidelity: tRNA discrimination, proofreading and induced fit. *Trends Biochem. Sci.* **26**, 124–130.
54. Chandra Sanyal, S. & Liljas, A. (2000) The end of the beginning: structural studies of ribosomal proteins. *Curr. Opin. Struct. Biol.* **10**, 633–636.
55. Cundliffe, E., Dixon, P., Stark, M., Stoffler, G., Ehrlich, R., Stoffler-Meilicke, M. & Cannon, M. (1979) Ribosomes in thiostrepton-resistant mutants of *Bacillus megaterium* lacking a single 50 S subunit protein. *J. Mol. Biol.* **132**, 235–252.
56. Gomez-Lorenzo, M.G., Spahn, C.M., Agrawal, R.K., Grassucci, R.A., Penczek, P., Chakraburtty, K., Ballesta, J.P., Lavandera, J.L., Garcia-Bustos, J.F. & Frank, J. (2000) Three-dimensional cryo-electron microscopy localization of EF2 in the *Saccharomyces cerevisiae* 80S ribosome at 17.5 Å resolution. *EMBO J.* **19**, 2710–2718.
57. Nikulin, A., Eliseikina, I., Tishchenko, S., Nevskaya, N., Davydova, N., Platonova, O., Piendl, W., Selmer, M., Liljas, A., Drygin, D., Zimmermann, R., Garber, M. & Nikonov, S. (2003) Structure of the L1 protuberance in the ribosome. *Nat. Struct. Biol.* **10**, 104–108.
58. Milligan R. A. & Unwin P. N. (1986) Location of exit channel for nascent protein in 80S ribosome. *Nature* **319**, 693–695.
59. Yonath, A., Leonard, K.R. & Wittmann, H.G. (1987) A tunnel in the large ribosomal subunit revealed by three-dimensional image reconstruction. *Science* **236**, 813–816.
60. Berisio, R., Schluenzen, F., Harms, J., Bashan, A., Auerbach, T., Baram, D. & Yonath, A. (2003) Structural insight into the role of the ribosomal tunnel in cellular regulation. *Nat. Struct. Biol.* **10**, 336–340.
61. Auerbach, T., Bashan, A., Harms, J., Schluenzen, F., Zarivach, R., Bartels, H., Agmon, I., Kessler, M., Pioletti, M., Franceschi, F. & Yonath, A. (2002) Antibiotics targeting ribosomes: crystallographic studies. *Curr. Drug Targets Infect. Disord.* **2**, 169–186.
62. Weisblum, B. (1995) Erythromycin resistance by ribosome modification. *Antimicrobial Agents Chemother.* **39**, 577–585.
63. Douthwaite, S., Hansen, L.H. & Mauvais, P. (2000) Macrolide-ketolide inhibition of MLS-resistant ribosomes is improved by alternative drug interaction with domain II of 23S rRNA. *Mol. Microbiol.* **36**, 183–193.
64. Periti, P., Mazzei, T., Mini, E. & Novelli, A. (1993) Adverse effects of macrolide antibacterials. *Drug Saf.* **9**, 346–364.
65. Chepkwony, H.K., Roets, E. & Hoogmartens, J. (2001) Liquid chromatography of troleandomycin. *J. Chromatogr. A* **914**, 53–58.
66. Unge, J., berg, A., Al-Kharadaghi, S., Nikulin, A., Nikonov, S., Davydova, N., Nevskaya, N., Garber, M. & Liljas, A. (1998) The crystal structure of ribosomal protein L22 from *Thermus thermophilus*: insights into the mechanism of erythromycin resistance. *Structure* **6**, 1577–1586.
67. Liao, S., Lin, J., Do, H. & Johnson, A.E. (1997) Both lumenal and cytosolic gating of the aqueous ER translocon pore are regulated from inside the ribosome during membrane protein integration. *Cell* **90**, 31–41.
68. Morris, D.R. & Geballe, A.P. (2000) Upstream open reading frames as regulators of mRNA translation. *Mol. Cell Biol.* **20**, 8635–8642.
69. Stroud, R.M. & Walter, P. (1999) Signal sequence recognition and protein targeting. *Curr. Opin. Struct. Biol.* **9**, 754–759.
70. Tenson, T. & Ehrenberg, M. (2002) Regulatory nascent peptides in the ribosomal tunnel. *Cell* **108**, 591–594.
71. Walter, P. & Johnson, A.E. (1994) Signal sequence recognition and protein targeting to the endoplasmic reticulum membrane. *Annu. Rev. Cell Biol.* **10**, 87–119.
72. Nakatogawa, H. & Ito, K. (2002) The ribosomal exit tunnel functions as a discriminating gate. *Cell* **108**, 629–636.
73. Sarker, S., Rudd, K.E. & Oliver, D. (2000) Revised translation start site for secM defines an atypical signal peptide that regulates *Escherichia coli* secA expression. *J. Bacteriol.* **182**, 5592–5595.
74. Gong, F. & Yanofsky, C. (2002) Instruction of translating ribosome by nascent peptide. *Science* **297**, 1864–1867.
75. Davydova, N., Streltsov, V., Wilce, M., Liljas, A. & Garber, M. (2002) L22 ribosomal protein and effect of its mutation on ribosome resistance to erythromycin. *J. Mol. Biol.* **322**, 635–644.
76. Gabashvili, I.S., Gregory, S.T., Valle, M., Grassucci, R., Worbs, M., Wahl, M.C., Dahlberg, A.E. & Frank, J. (2001) The polypeptide tunnel system in the ribosome and its gating in erythromycin resistance mutants of L4 and L22. *Mol. Cell.* **8**, 181–188.